The Astrophysical Journal, 610:510–522, 2004 July 20

HEAVY-ELEMENT ABUNDANCES IN SOLAR ENERGETIC PARTICLE EVENTS

D. V. Reames and C. K. Ng[1]
NASA Goddard Space Flight Center, Code 661, Greenbelt, MD 20771; reames@milkyway.gsfc.nasa.gov, cheeng@milkyway.gsfc.nasa.gov
Received 2004 February 25; accepted 2004 March 29

ABSTRACT

We survey the relative abundances of elements with $1 \leq Z \leq 82$ in solar energetic particle (SEP) events observed at 2–10 MeV amu^{-1} during nearly 9 years aboard the *Wind* spacecraft, with special emphasis on enhanced abundances of elements with $Z \geq 34$. Abundances of Fe/O again show a bimodal distribution with distinct contributions from impulsive and gradual SEP events, as seen in earlier solar cycles. Periods with greatly enhanced abundances of $(50 \leq Z \leq 56)$/O, just as those with enhanced ^{3}He/^{4}He, fall prominently in the Fe-rich population of the impulsive SEP events. In a sample of the 39 largest impulsive events, 25 have measurable enhancements in $(50 \leq Z \leq 56)$/O and $(76 \leq Z \leq 82)$/O, relative to coronal values, ranging from ~100 to 10,000. By contrast, in a sample of 45 large gradual events the corresponding enhancements vary from ~0.2 to 20. However, the magnitude of the heavy-element enhancements in impulsive events is less striking than their strong correlation with the Fe spectral index and flare size, with *the largest enhancements occurring in flares with the steepest Fe spectra, the smallest Fe fluence, and the lowest X-ray intensity*, as reported here for the first time. Thus, it seems that small events with low energy input can produce only steep spectra of the dominant species but accelerate rare heavy elements with great efficiency, probably by selective absorption of resonant waves in the flare plasma. With increased energy input, enhancements diminish as heavy ions are depleted, and spectra of the dominant species harden.

Subject headings: acceleration of particles — shock waves — Sun: abundances — Sun: coronal mass ejections (CMEs) — Sun: flares — Sun: particle emission

1. INTRODUCTION

Relative abundances of elements and isotopes have proven to be a rich source of information on the origin and history of the populations of energetic ions that we have encountered throughout the heliosphere (e.g., Reames 1999). In solar energetic particle (SEP) events, abundances have aided in distinguishing two underlying mechanisms of particle acceleration that contribute to "gradual" and "impulsive" SEP events (see the reviews by Reames 1990, 1995b, 1999, 2002; Kahler 1992, 1994, 2001; Gosling 1993; Lee 1997; Tylka 2001). In the large gradual SEP events, abundances of elements up to Fe at a few MeV amu^{-1} are, on average, similar to those of the solar corona and solar wind (Meyer 1985; Reames 1995a, 1999), from which ions are accelerated by shock waves driven out from the Sun by coronal mass ejections (CMEs). In contrast, the impulsive SEP events associated with solar flares have thousandfold enhancements of ^{3}He/^{4}He and enhancements in heavier elements that increase with decreasing charge-to-mass ratio Q/A of the ions at coronal temperatures (e.g., Reames et al. 1994). The pattern of enhancements in impulsive SEP events is generally believed to result from resonant wave-particle interactions in the turbulent flare plasma (Fisk 1978; Temerin & Roth 1992; Miller & Viñas 1993; Roth & Temerin 1997; Miller 1998). In some large SEP events, however, intermediate abundances may result when remnant suprathermal ions from impulsive events contribute to the material accelerated by CME-driven shock waves (Mason et al. 1999; Tylka et al. 2001; Desai et al. 2003). In addition, the effects of particle transport from the source can cause abundances to vary with particle energy and with space and time during gradual events (Ng et al. 2003).

For elements with atomic number $Z \geq 34$, solar abundances decrease precipitously by as much as ~6–8 orders of magnitude below that of O (Grevesse & Sauval 1998), and early instruments were unable to collect enough ions to make regular measurements of abundances in this region. The earliest measurements of heavy-element abundances in SEP events were made using particle tracks collected in a glass window of the *Apollo 16* command module (Shirk & Price 1973). In recent years, however, regular measurements of the abundances of elements throughout the periodic table above Fe have begun to contribute to the study of SEP events (Reames 2000; Reames et al. 2001; Tylka et al. 2002; Mason et al. 2004). For impulsive events, Q/A-dependent enhancements continue into the region of heavy elements, producing approximately thousandfold enhancements for $(Z \geq 50)$/O. For gradual events, however, ions with $Z \geq 34$ often have coronal abundances or only modest enhancements that follow a temporal behavior similar to that of Fe/O and show high-energy spectral rollovers with the same Q/A-dependence as the elements up through Fe (Reames et al. 2001). Most of the recent measurements of ions with $34 \leq Z \leq 82$ mentioned above have been made in the 3.3–10 MeV amu^{-1} region with the large-geometry Low-Energy Matrix Telescope (LEMT) on the *Wind* spacecraft, which we discuss herein. Recently, however, time-of-flight–based measurements in the 0.1–1 MeV amu^{-1} region showing similar heavy-element enhancements in ^{3}He-rich events have been reported by Mason et al. (2004).

The previous heavy-element observations from LEMT were reported for limited time periods or in selected SEP events. In this paper we extend those results significantly by surveying all such measurements from 1994 November 4 through 2003 September 28. This allows us to study the statistical properties

[1] Also at Department of Astronomy, University of Maryland, College Park, MD 20742.

of heavy-element abundances in a large sample of SEP events of various kinds. Properties of the LEMT telescope have been described by von Rosenvinge et al. (1995), and its response to heavy elements has been described in detail by Reames (2000).

2. THE SYNOPTIC VIEW

A classical way to provide an overall view of the systematic variations of element and isotopic abundances has been to divide the entire sample period into daily averages and plot the pattern of intensities of one species against another on a day-to-day basis. This technique allows one to view the full sweep of abundance variations with no bias as to the selection of "events" for study; each day is an "event." Reames (1988) made plots of daily averaged Fe versus O at $\sim$2 MeV amu^{-1} and found a bimodal distribution corresponding to the presence of impulsive and gradual SEP events. Distinguishing the points in the plot of Fe versus O by their corresponding ^{3}He/^{4}He, proton/electron, or He/H ratios, the underlying properties of the contributing impulsive and gradual events were further identified.

Owing to the greater sensitivity of LEMT, we have divided the present data set into 8 hr intervals and show in Figure 1 the Fe versus O intensities for each of those intervals in the $\sim$9 year study period. In the top panel of the figure, the color and size of the symbols varies with the ^{3}He/^{4}He ratio at 2.1–2.5 MeV amu^{-1} during each interval, while symbols in the bottom panel depend on the $(50 \leq Z \leq 56)$/O abundance ratio at 3.3–10 MeV amu^{-1}. The approximate intensity of background anomalous cosmic ray (ACR) O during solar minimum is marked on the panels. This represents an approximate lower bound for the O intensity for the years 1994–1998 (see Reames & McDonald 2003), during which many small SEP events occurred. Each panel in Figure 1 contains about 4900 points.

In Figure 1 (*top*) it is not difficult to follow the loci of the distributions that we identify with impulsive and gradual SEP events at or slightly above the lines of Fe/O = 1 and 0.1, respectively. The ^{3}He-rich intervals cluster near the line of Fe/O = 1 at moderate intensities but are deflected below that line at very low intensities, when background from ACR O is present to depress Fe/O from the impulsive events. At higher intensities of Fe or O, ^{3}He/^{4}He in impulsive events decreases to values below 0.2, which are not easily measured by LEMT because of its limited resolution (Reames et al. 1997). However, the track of impulsive event intervals seems to end where the intensities of Fe or O reach $\sim 10^{-2}$ particles cm^{-2} sr^{-1} s^{-1} MeV^{-1} amu. Intervals during gradual events are distributed about the line Fe/O = 0.1 at low and moderate intensities but generally rise above Fe/O = 0.1 at high intensities; many of these high-intensity intervals occur early during large SEP events when Fe/O is elevated by transport-dominated effects (e.g., Tylka et al. 1999; Ng et al. 1999; Reames et al. 2000), including those in the large "Bastille Day" event of 2000 July 14 (Reames et al. 2001). Note that, at the very lowest Fe intensities, a few of the 8 hr intervals distributed near Fe/O $\sim$ 0.1 actually correspond to ions from corotating interacting regions for which abundances are also unenhanced (see, e.g., Reames 1999).

In Figure 1 (*bottom*) $(50 \leq Z \leq 56)$/O ratios highlight the points. Intervals with large values of this ratio are seen to cluster along the track of Fe/O = 1. At the lowest intensities, of course, elements with $50 \leq Z \leq 56$ can only be seen when these ions are greatly enhanced relative to the coronal $(50 \leq Z \leq 56)$/O ratio, taken as 2.90×10^{-6} (Grevesse & Sauval 1998; see Reames 2000). Near the top of the impulsive region where Fe or O reach $\sim 10^{-2}$ particles cm^{-2} sr^{-1} s^{-1} MeV^{-1} amu, near-coronal abundances of $(50 \leq Z \leq 56)$/O would be measurable, but hundredfold and thousandfold enhancements of $(50 \leq Z \leq 56)$/O are seen. These large enhancements along the impulsive track contrast with the nearly coronal values in the gradual region nearby. Occasional instances of significantly enhanced $(50 \leq Z \leq 56)$/O in the gradual population (Fe/O $\sim$ 0.1) at intermediate intensities usually correspond to intervals in which both impulsive and gradual events contribute, as we see in § 4 below.

Superficially, it may seem that ^{3}He and $Z \geq 50$ ion enhancements occupy nearly exclusive regions of the Fe/O $\sim$ 1, impulsive-event track. However, instrument sensitivity limits the observation of even greatly enhanced $Z \geq 50$ ions in small events, and ^{3}He/^{4}He ratios decrease in large events, probably because the supply of ^{3}He ions in the flare volume is becoming exhausted (Reames 1999). These two facts conspire to limit the observational overlap of ^{3}He and $Z \geq 50$ ion enhancements. We believe that the apparent separation of impulsive events with ^{3}He and $Z \geq 50$ enhancements is *entirely* instrumental.

Finally, we point out that the 8 hr averaging of the data in Figure 1 distorts the relative probability of impulsive and gradual events. Gradual events, lasting several days, are sampled several times, while more than one impulsive event may contribute to a single point in the figure.

3. IMPULSIVE EVENTS

3.1. *Preliminary Impulsive Event Selection*

To place the heavy-element abundances in the general context of impulsive events, we have begun by scanning hourly averaged data to select a preliminary list of events using two different criteria: (1) events in which ^{3}He/^{4}He > 0.5 and intensities of ^{3}He or ^{4}He exceed 10^{-4} particles cm^{-2} sr^{-1} s^{-1} MeV^{-1} amu and (2) events in which Fe/O > 0.5 and intensities of Fe exceed 10^{-5} particles cm^{-2} sr^{-1} s^{-1} MeV^{-1} amu. The second criterion for impulsive events is clearly guided by the distributions of particle abundances shown in Figure 1. A total of 133 events were found, 80 met the ^{3}He-rich criteria, 82 met the Fe-rich criteria, and 29 met both criteria. Note that ^{3}He-rich events can occur in intervals that need not contribute to Figure 1, because the events are too small to have measurable Fe and O intensities. Relaxing the criteria on the intensities of ^{3}He and ^{4}He or their ratio would have produced hundreds of candidate events. However, determining whether intensity increases are truly new event onsets becomes difficult for smaller events, so we have used conservative criteria.

Intensity-time profiles for events with a variety of properties are compared in Figure 2. Events 1 and 2 in the figure are ^{3}He-rich (^{3}He/^{4}He $\sim$10) events of moderate intensity, for which the intensities of Fe and O are too low for measurement. The latter is completely obscured by the ACR O that runs across the panel. Events 3 and 4 are somewhat larger, although they occur in a high background of H and ^{4}He from a gradual event much earlier. These events have similar intensities of ^{3}He, but event 4 has more ^{4}He and clear increases in O and Fe. Event 5 is similar to event 4 but shows a small increase of associated heavy elements. Events 6 and 7 have higher intensities of ^{4}He, Fe, and O and significant numbers of heavy elements. ^{3}He/^{4}He is substantially reduced in both events, although it is measurable in event 7. Events 8 and 9 have similar intensities of H, ^{4}He, O, and Fe, but event 9 has a substantial

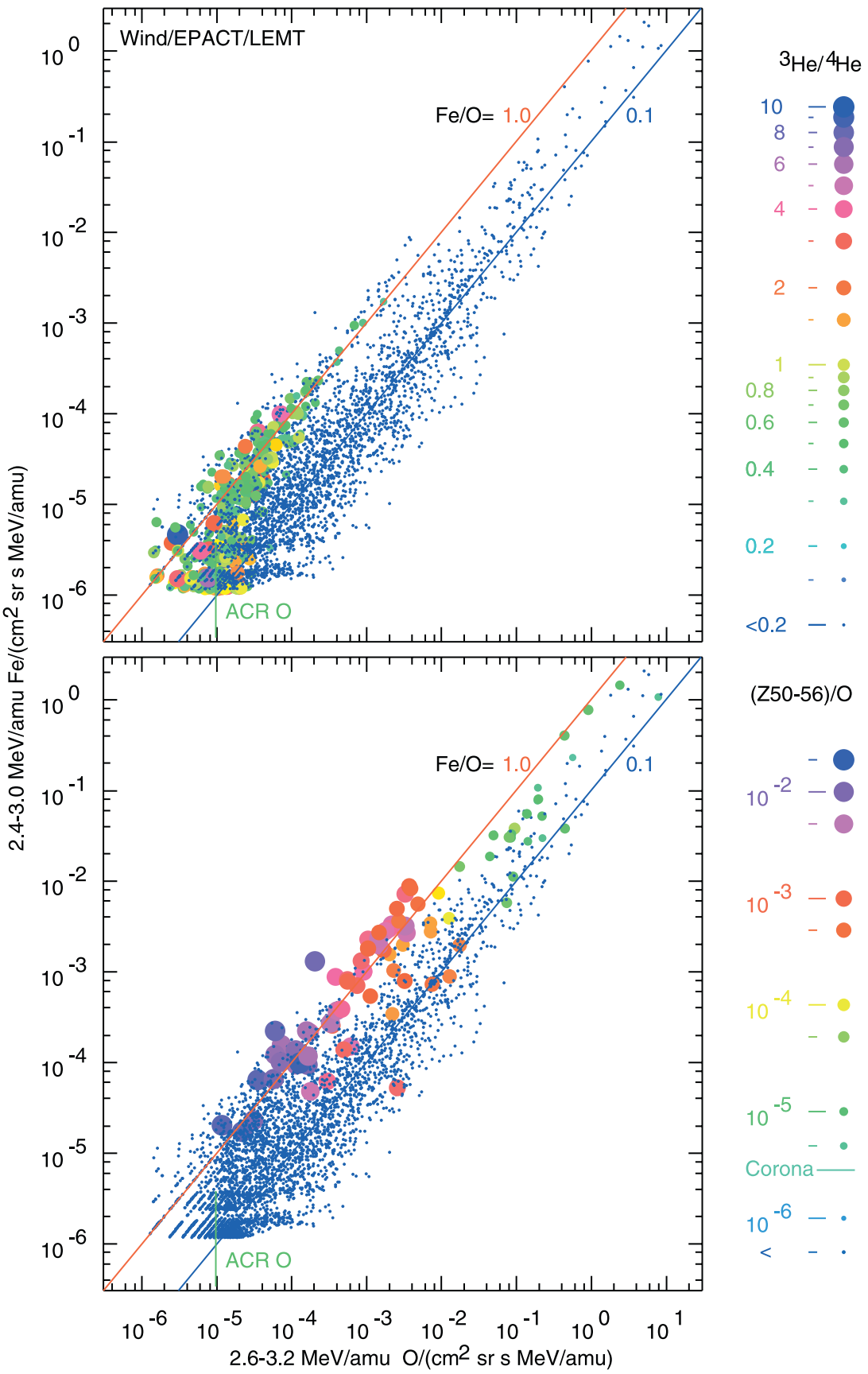

FIG. 1.—In both panels, particle intensities of Fe plotted vs. those of O for all 8 hr intervals in the 9 year study period in which Fe and O were measurable. The indicated intensity of ACR O forms a lower bound on the O intensity during solar minimum. The symbols used for data in the top panel indicate the average value of ^{3}He/^{4}He during each interval, as indicated in the scale to the right of the panel. Symbols in the bottom panel denote the $(50 \leq Z \leq 56)$/O abundance ratio as shown in the right-hand scale. Lines drawn along Fe/O = 1 and 0.1 approximately track the loci expected for impulsive and gradual SEP events.

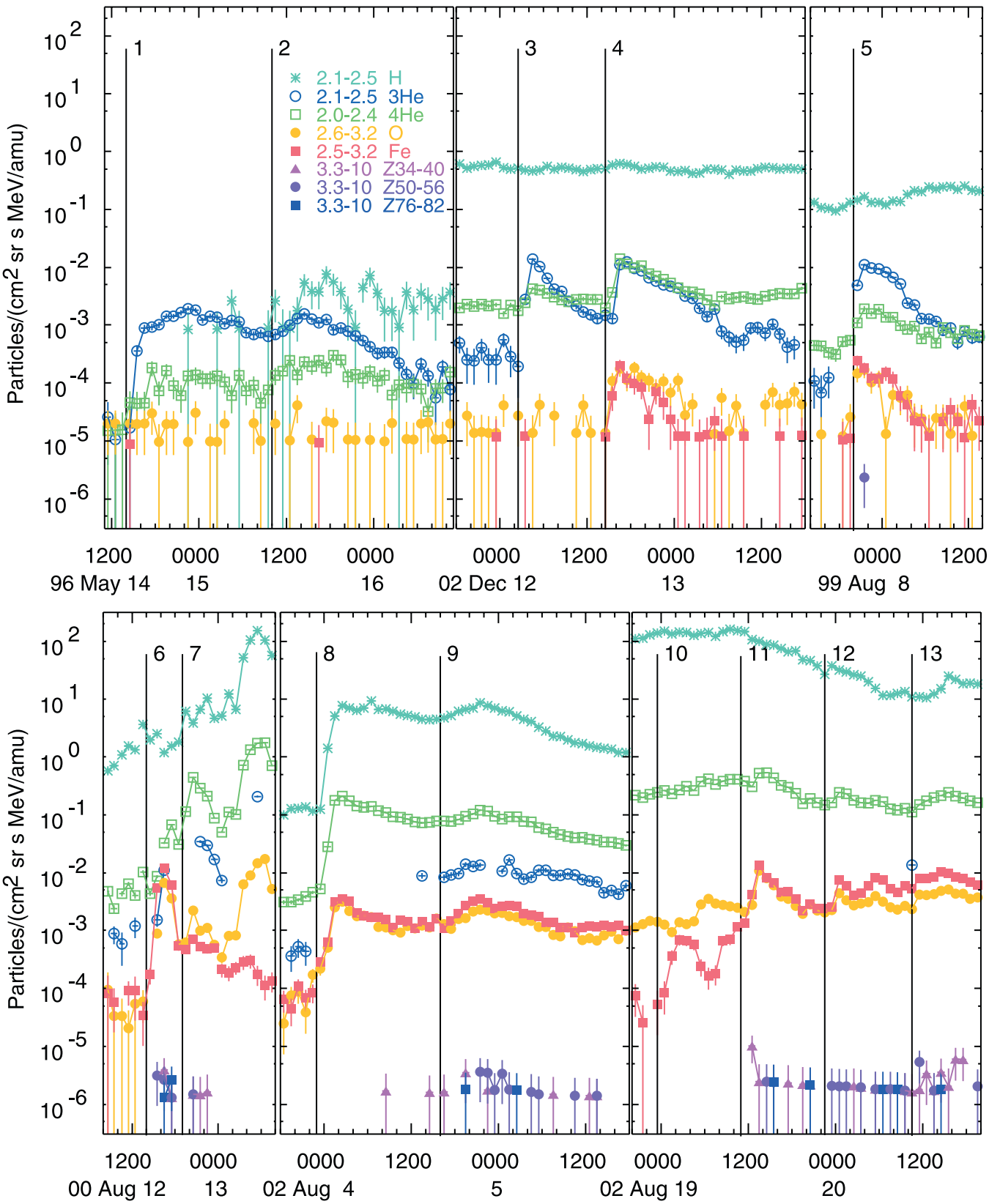

FIG. 2.—Intensities of various ion species vs. time, compared for 13 impulsive SEP events spanning a wide variety of intensities and element abundances (see text).

TABLE 1

LARGE IMPULSIVE SEP EVENTS

Event	SEP Onset Time	^{3}He/^{4}He	Fe Fluence[a] (cm^{-2} sr^{-1} MeV^{-1} amu)	Fe Spectral Index	O Spectral Index	Fe/O Enhancement[b]	$(34 \leq Z \leq 40)$/O Enhancement[c]	$(50 \leq Z \leq 56)$/O Enhancement[d]	$(76 \leq Z \leq 82)$/O Enhancement[e]
1.....	1997 Sep 18 0300	0.67 ± 0.1	11.3 ± 0.6	3.40 ± 0.2	3.17 ± 0.15	6.6 ± 0.48	<71	548 ± 548	<1570
2.....	1997 Sep 18 2300	0.81 ± 0.1	7.16 ± 0.48	3.62 ± 0.13	2.72 ± 0.09	5.11 ± 0.48	99 ± 99	<759	<2170
3.....	1998 Sep 6 0900	<0.2	9.30 ± 0.59	2.36 ± 0.17	2.27 ± 0.12	11.4 ± 1.0	<108	1660 ± 1170	<2370
4.....	1998 Sep 9 0700	<0.2	48.8 ± 1.4	2.92 ± 0.21	3.13 ± 0.10	8.45 ± 0.31	19 ± 19	<144	<413
5.....	1998 Sep 26 1900	<0.2	54.5 ± 1.8	3.8 ± 0.20	4.43 ± 0.14	9.51 ± 0.51	109 ± 77	1260 ± 727	<1200
6.....	1998 Sep 27 1100	<0.2	76.9 ± 2.1	3.17 ± 0.22	3.78 ± 0.16	5.96 ± 0.20	76 ± 34	929 ± 329	997 ± 576
7.....	1998 Sep 27 2000	<0.2	64.2 ± 1.9	3.33 ± 0.24	3.91 ± 0.13	11.8 ± 0.5	68 ± 48	1830 ± 693	<747
8.....	1998 Sep 28 0300	<0.2	62 ± 1.8	3.37 ± 0.19	3.66 ± 0.11	10.9 ± 0.5	66 ± 47	<254	727 ± 727
9.....	1998 Sep 28 1000	<0.2	51.8 ± 1.6	3.53 ± 0.18	4.24 ± 0.13	13.5 ± 0.7	166 ± 96	1280 ± 738	1220 ± 1220
10.....	1998 Sep 29 0700	<0.2	23.6 ± 1.0	3.57 ± 0.29	3.99 ± 0.13	7.19 ± 0.42	<56	431 ± 431	1230 ± 1230
11.....	1999 Feb 20 0600	<0.2	4.18 ± 0.39	3.42 ± 0.22	3.19 ± 0.17	36.1 ± 8.4	<1220	<9350	<26800
12.....	1999 Feb 20 1700	<0.2	7.95 ± 0.53	3.48 ± 0.25	3.59 ± 0.28	23.3 ± 3.1	<403	<3090	<8840
13.....	1999 Jun 18 1500	0.23 ± 0.1	11.8 ± 0.8	2.77 ± 0.17	2.84 ± 0.14	8.29 ± 0.73	<108	<831	<2380
14.....	1999 Aug 7 2000	5.4 ± 0.3	3.58 ± 0.38	4.38 ± 0.39	4.11 ± 0.31	8.51 ± 1.59	<670	10300 ± 7380	<14700
15.....	1999 Nov 16 0900	<0.2	5.97 ± 0.49	3.92 ± 0.10	3.63 ± 0.32	10.2 ± 1.6	<419	<3210	<9190
16.....	1999 Dec 24 0500	<0.2	6.97 ± 0.54	2.86 ± 0.13	2.97 ± 0.17	10.9 ± 1.3	225 ± 226	<1730	<4940
17.....	1999 Dec 27 0700	0.2 ± 0.1	13.7 ± 0.7	2.96 ± 0.19	3.38 ± 0.42	22.6 ± 2.3	<234	1800 ± 1800	<5140
18.....	2000 Mar 7 1500	<0.2	9.46 ± 0.61	2.88 ± 0.18	2.7 ± 0.1	16.9 ± 1.8	<186	<1430	<4090
19.....	2000 Mar 8 0300	0.23 ± 0.1	7.51 ± 0.54	2.51 ± 0.16	2.99 ± 0.14	8.65 ± 0.80	<132	1010 ± 1010	<2890
20.....	2000 May 1 1100	<0.2	80.6 ± 1.9	2.96 ± 0.08	2.94 ± 0.11	17 ± 0.7	<32	737 ± 426	<702
21.....	2000 May 4 1400	<0.2	4.89 ± 0.44	2.3 ± 0.20	2.29 ± 0.10	14.2 ± 1.6	<193	<1480	<4230
22.....	2000 May 23 1730	0.24 ± 0.1	6.79 ± 0.63	3.28 ± 0.21	4.04 ± 0.11	8.12 ± 1.13	<304	2330 ± 2340	<6670
23.....	2000 May 24 0030	0.33 ± 0.1	71.6 ± 1.9	3.42 ± 0.15	3.93 ± 0.13	8.1 ± 0.31	24 ± 24	365 ± 259	<523
24.....	2000 Jun 4 0900	0.23 ± 0.1	4.15 ± 0.43	3.2 ± 0.35	3.56 ± 0.25	13.9 ± 2.2	<503	<3850	<11000
25.....	2000 Jun 4 1400	0.29 ± 0.1	11 ± 0.7	4.07 ± 0.13	4.68 ± 0.29	10.3 ± 1.2	276 ± 277	<2120	<6060
26.....	2000 Aug 12 1400	<0.2	92.5 ± 2.2	4.07 ± 0.15	4.13 ± 0.07	16.4 ± 0.8	199 ± 100	1900 ± 854	3270 ± 1890
27.....	2000 Dec 28 0100	0.66 ± 0.1	9.07 ± 0.61	3.27 ± 0.18	4.01 ± 0.25	9.43 ± 1.0	<207	1580 ± 1590	<4530
28.....	2001 Apr 14 1800	<0.2	123 ± 2.6	2.77 ± 0.16	3.07 ± 0.12	10.8 ± 0.3	145 ± 46	999 ± 334	<318
29.....	2001 Sep 10 1700	<0.2	24.1 ± 1.0	2.68 ± 0.19	2.81 ± 0.18	11.9 ± 0.7	51 ± 51	391 ± 391	<1120
30.....	2001 Sep 11 1400	0.41 ± 0.1	33.1 ± 1.2	3.28 ± 0.20	3.62 ± 0.18	9.7 ± 0.52	50 ± 50	382 ± 382	<1090
31.....	2002 Apr 15 0000	<0.2	2.76 ± 0.36	3.49 ± 0.16	2.87 ± 0.22	5.9 ± 1.1	<394	<3020	<8650
32.....	2002 Apr 15 0500	0.34 ± 0.1	21.8 ± 1.0	3.26 ± 0.18	3.57 ± 0.16	7.68 ± 0.52	142 ± 100	<543	<1550
33.....	2002 Aug 3 2300	<0.2	96.8 ± 2.3	2.48 ± 0.13	2.55 ± 0.08	9.18 ± 0.29	26 ± 19	<101	<290
34.....	2002 Aug 4 1600	<0.2	127 ± 2.7	3.00 ± 0.14	3.03 ± 0.11	10.4 ± 0.3	78 ± 35	1200 ± 380	687 ± 486
35.....	2002 Aug 18 2330	<0.2	10.6 ± 1.1	2.34 ± 0.26	3.69 ± 0.15	3.00 ± 0.27	<75	<577	<1650
36.....	2002 Aug 19 1100	<0.2	185 ± 3.9	1.90 ± 0.17	2.33 ± 0.16	10 ± 0.3	68 ± 24	130 ± 92	373 ± 264
37.....	2002 Aug 19 2230	<0.2	214 ± 3.9	2.43 ± 0.16	2.82 ± 0.09	15.8 ± 0.5	42 ± 24	636 ± 260	606 ± 429
38.....	2002 Aug 20 1030	<0.2	494 ± 6.1	1.80 ± 0.10	1.88 ± 0.06	14.6 ± 0.3	66 ± 16	252 ± 89	90 ± 90
39.....	2002 Sep 27 0400	0.25 ± 0.1	2.86 ± 0.32	2.61 ± 0.16	2.30 ± 0.16	3.33 ± 0.40	96 ± 96	<735	<2100

[a] At 2.4–3.2 MeV amu^{-1}.
[b] At 3.3–10 MeV amu^{-1}, relative to coronal (Fe/O = 0.134).
[c] At 3.3–10 MeV amu^{-1}, relative to coronal $[(34 \leq Z \leq 40)/O = 2.22 \times 10^{-5}]$.
[d] At 3.3–10 MeV amu^{-1}, relative to coronal $[(50 \leq Z \leq 56)/O = 2.90 \times 10^{-6}]$.
[e] At 3.3–10 MeV amu^{-1}, relative to coronal $[(76 \leq Z \leq 82)/O = 1.01 \times 10^{-6}]$.

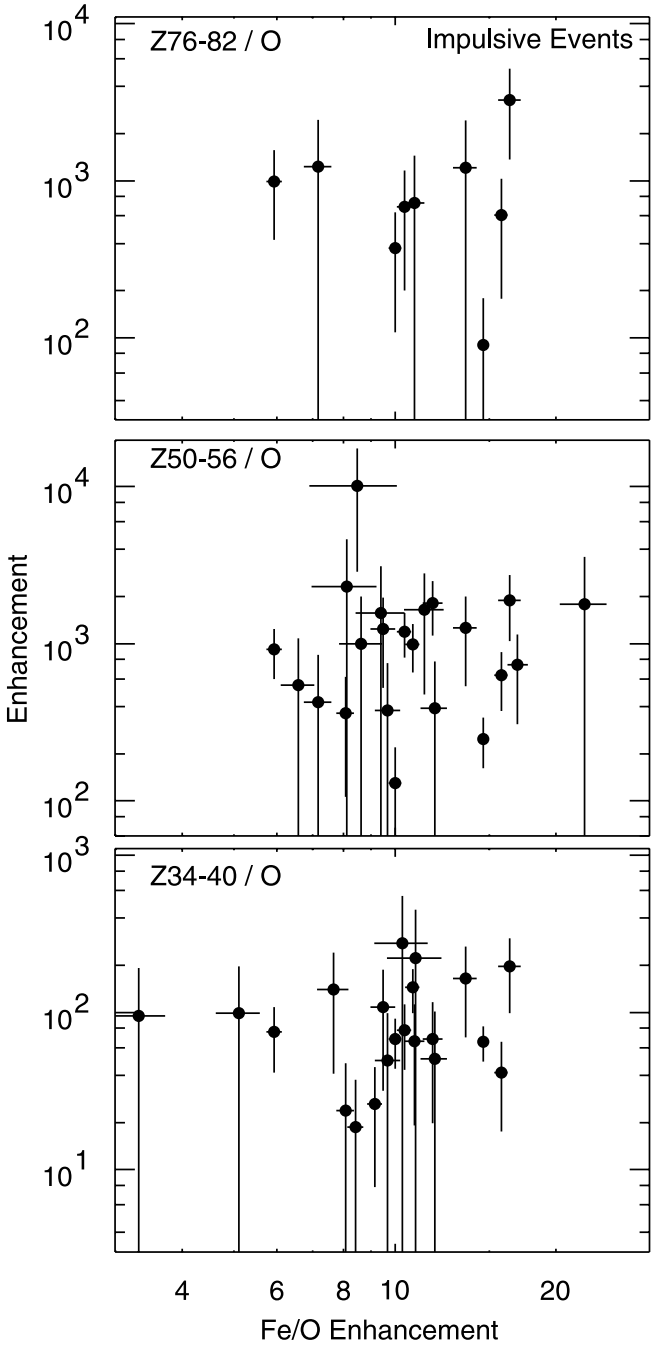

FIG. 3.—Enhancements in the heavy-element abundance ratios $(34 \leq Z \leq 40)/O$, $(50 \leq Z \leq 56)/O$, and $(76 \leq Z \leq 82)/O$ relative to coronal abundance ratios, shown vs. the corresponding enhancement in Fe/O for a sample of 39 large impulsive events.

number of heavy ions and measurable ^{3}He. Events 10–13 are a series of large impulsive events that sometimes occur when the spacecraft is inside the CME following a gradual event and is thus magnetically well connected to an active region where flares are likely (see Reames 2000 for a similar example).

The rate of occurrence of impulsive events increases with the solar cycle (e.g., Reames et al. 1994). However, near solar maximum these small events are obscured by the presence of large gradual events. During the years 2000–2002, for example, the 2.6–3.2 MeV amu^{-1} O intensity is above 10^{-4} particles cm^{-2} sr^{-1} s^{-1} MeV^{-1} amu for 37% of the time, making it difficult to see and measure Fe and O in impulsive events with this intensity or less. During the same 3 years the 2.0–2.4 MeV amu^{-1} ^{4}He intensity is above 10^{-3} particles cm^{-2} sr^{-1} s^{-1} MeV^{-1} amu for 68% of the time, making the observation of small ^{3}He-rich events even more difficult. During these years, the 2.1–2.5 MeV H intensity is above the extremely high value of 1 particle cm^{-2} sr^{-1} s^{-1} MeV^{-1} for 43% of the time.

3.2. *Large Impulsive Events: Abundances*

Clearly, as seen from Figure 1, heavy ions are most likely to be found in the most intense Fe-rich impulsive SEP events. Therefore, from the original sample of Fe-rich impulsive events we select a subset of "large" impulsive events with Fe intensity above 10^{-4} particles cm^{-2} sr^{-1} s^{-1} MeV^{-1} amu. Properties of the 39 large impulsive events selected are shown in Table 1. Of the 39 events, 33 events have $Z \geq 34$ ions, and 25 events have $Z \geq 50$ ions. (*All* of the 14 events with Fe intensity above 10^{-3} particles cm^{-2} sr^{-1} s^{-1} MeV^{-1} amu have heavy elements.)

In Figure 3 we show the time-integrated heavy-element enhancements as a function of the corresponding enhancement of Fe/O for the sample of 39 large impulsive events defined above. The coronal abundance ratios for Fe/O, $(34 \leq Z \leq 40)/O$, $(50 \leq Z \leq 56)/O$, and $(76 \leq Z \leq 82)/O$ are taken as 0.134, 2.22×10^{-5}, 2.90×10^{-6}, and 1.01×10^{-6}, respectively. The enhancement factors cluster around ~10, ~100, ~1000, and ~1000 for the four species, respectively, and there is little evidence of any correlated behavior when we consider only impulsive events. This is consistent with the poor correlations found in the event-to-event abundance variations for elements up to Fe (Reames et al. 1994).

To summarize the heavy-element abundances in impulsive events, we have averaged the element abundances over all 39 large impulsive-event periods, whether they had heavy elements or not. The average abundance enhancements of the elements in these events are shown in Figure 4 as filled circles as functions of Z and of Q/A using the equilibrium Q at a temperature of ~3 MK. The open circles in Figure 4 supplement these measurements with the average enhancements of other elements determined in the same energy range in earlier studies of impulsive events (Reames et al. 1994; Reames 1995a, 1999). Ionization states at a coronal temperature of ~3 MK have been shown to organize element abundances in impulsive events (Reames et al. 1994). Values of Q at a temperature of ~3 MK for the elements were found from Arnaud & Rothenflug (1985) for $Z < 26$, from Arnaud & Raymond (1992) for $Z = 26$, and from Post et al. (1977) for $Z > 26$.

3.3. *Large Impulsive Events: Spectra*

Figure 5 shows energy spectra for ^{4}He, C, O, Ne, Si, and Fe, and for ions with $34 \leq Z \leq 40$ and $50 \leq Z \leq 56$ in three of the large impulsive SEP events that have significant intensities of heavy elements. The spectra of different elements can be seen to differ in slope within a given event, and to some extent they depart from a power-law behavior. This is not surprising, since theoretical spectra (Miller 1998) and theoretical fits to observations (Mason et al. 2002) have shown complex behavior. However, to illustrate the range of variation, we find least-squares power-law spectral indexes for ^{4}He, C, O, Ne, Si, Fe, and $34 \leq Z \leq 40$ of -2.59 ± 0.18, -3.10 ± 0.12, -3.17 ± 0.12, -3.33 ± 0.16, -3.04 ± 0.13, -2.77 ± 0.16, and -2.17 ± 0.71, respectively, in the 2001 April 14 event. The corresponding spectral indexes for the 2002 August 20 event

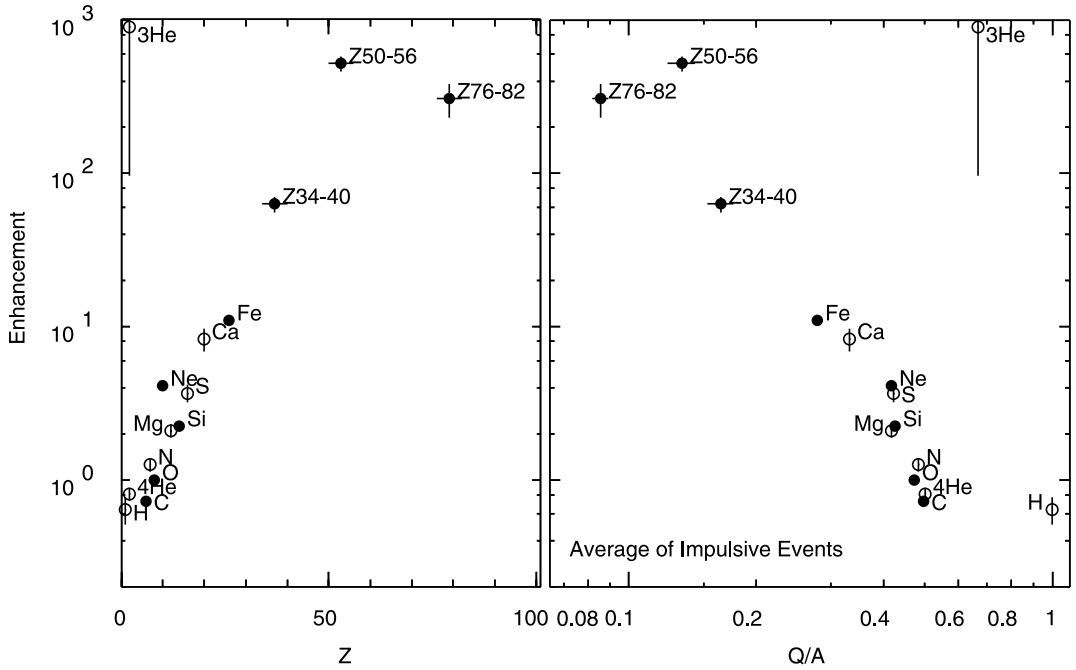

FIG. 4.—Abundance enhancements in average large impulsive events relative to coronal abundances, shown as a function of Z and of Q/A at ~3 MK for the present study (*filled circles*) and for other elements measured in previous studies (*open circles*) (see text).

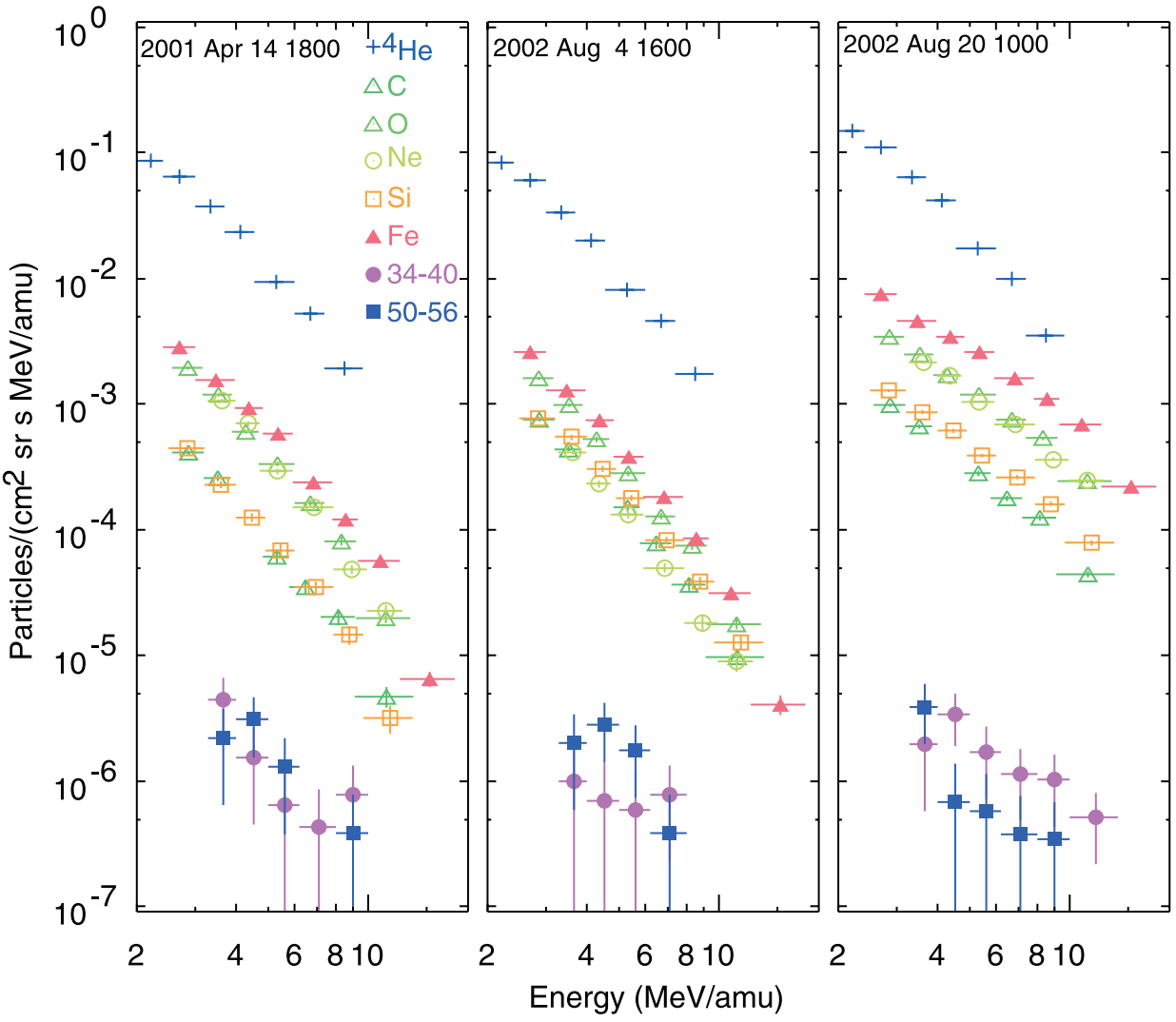

FIG. 5.—Energy spectra for ^{4}He, C, O, Ne, Si, and Fe, and for ions with $34 \leq Z \leq 40$ and $50 \leq Z \leq 56$ in three impulsive SEP events with measurable heavy elements.

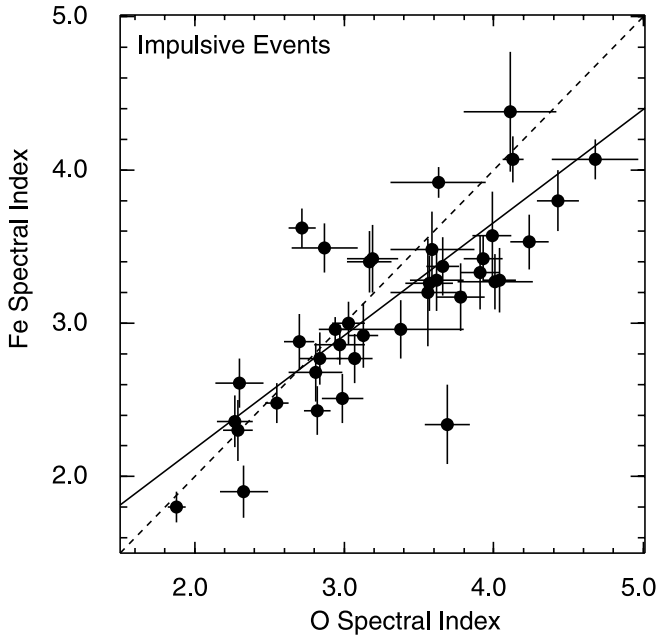

FIG. 6.—Cross-plot of the absolute values of the power-law spectral indexes of O and Fe for the 39 large impulsive SEP events of our study. The least-squares fit (*solid line*) is shown, and the dashed line identifies events with equal Fe and O spectral indexes. The spectra of Fe tend to be flatter than those of O, especially when both spectra are steep.

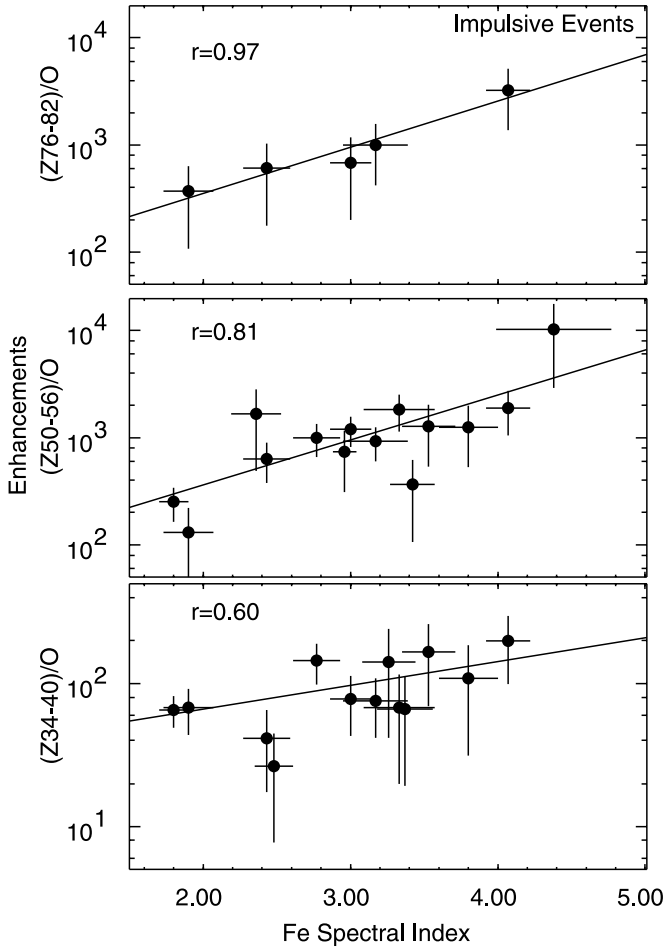

FIG. 7.—Enhancements in the $(34 \leq Z \leq 40)/O$, $(50 \leq Z \leq 56)/O$, and $(76 \leq Z \leq 82)/O$ abundances relative to the corona, shown as a function of the Fe spectral index for the large impulsive events in which the abundances are well determined. The correlation coefficients and least-squares fit lines are shown.

are -2.51 ± 0.16, -2.15 ± 0.08, -1.88 ± 0.06, -1.93 ± 0.07, -1.91 ± 0.06, -1.80 ± 0.11, and -1.50 ± 0.33. A difference in the spectra of different elements means that their relative abundances, and enhancements, will vary with energy. For these two events there is a tendency for $(34 \leq Z \leq 40)/O$ to rise almost linearly with energy, although the errors in this determination are large.

The sample spectra above show considerable variation in spectral slope among the species shown. In particular, they suggest that the spectrum of Fe can be harder than that of O in an event, and perhaps the spectra of heavier ions can be harder than the spectra of Fe. Measurement statistics do not allow us to study the systematic behavior of heavy-element spectra, but we can compare the spectral indexes of Fe and O in all 39 large impulsive events (see Table 1), as shown in Figure 6. Most events fall below the dashed diagonal line in the figure, showing that Fe spectra are systematically harder than O spectra. As the spectra become softer, the points fall increasingly below the diagonal line, and the difference between Fe and O becomes greater. This trend is also shown by the solid least-squares fit line.

Armed with this information on the impulsive event spectra, we plot in Figure 7 the enhancements in the $(34 \leq Z \leq 40)/O$, $(50 \leq Z \leq 56)/O$, and $(76 \leq Z \leq 82)/O$ abundances, relative to the corona, as a function of the Fe spectral index for the large impulsive events. For clarity we have omitted from the figure events with abundances that are only upper limits or have large errors. A high degree of correlation is seen in the figure, and the correlation coefficients increase as Z of the heavy elements increases. Poorer correlations are found when the spectral index of O replaces that of Fe.

Anticipating that steep spectra might be associated with small events with reduced energy input, we plot in Figure 8 (*left*) events with well-determined enhancement in $(50 \leq Z \leq 56)/O$ versus the Fe fluence. Of course, the fluence will depend on how magnetically well connected the events are, and in a few cases the time integration of Fe is truncated by the onset of a new event. Nevertheless, small events have greater enhancements of $(50 \leq Z \leq 56)/O$. The enhancements are plotted versus the NOAA *GOES* soft X-ray peak flux for each event in Figure 8 (*right*). Most of the events come from C- and M-class flares. Soft X-rays represent heating of the flare plasma, which is more sensitive to the acceleration of electrons than that of ions. Nevertheless, a substantial correlation is found here as well. Reames et al. (1988) found a similar behavior for $^3He/^4He$ in impulsive events; $^3He/^4He$ decreased as hard and soft X-ray fluxes and Km type III radio intensities increased.

4. GRADUAL EVENTS

For comparison with the impulsive events described above, we have selected a sample of large gradual events. Guided by Figure 1, we chose as gradual all events in which the intensity of 2.6–3.2 MeV amu^{-1} O exceeded 10^{-2} particles cm^{-2} sr^{-1} s^{-1} MeV^{-1} amu; 48 large events met this criterion. Properties of these events are shown in Table 2.

Figure 9 shows intensities of various ion species and enhancements relative to coronal abundances for Fe/O, $(34 \leq Z \leq 40)/O$, and $(50 \leq Z \leq 56)/O$ as a function of time during three gradual events. These events, from CME sources

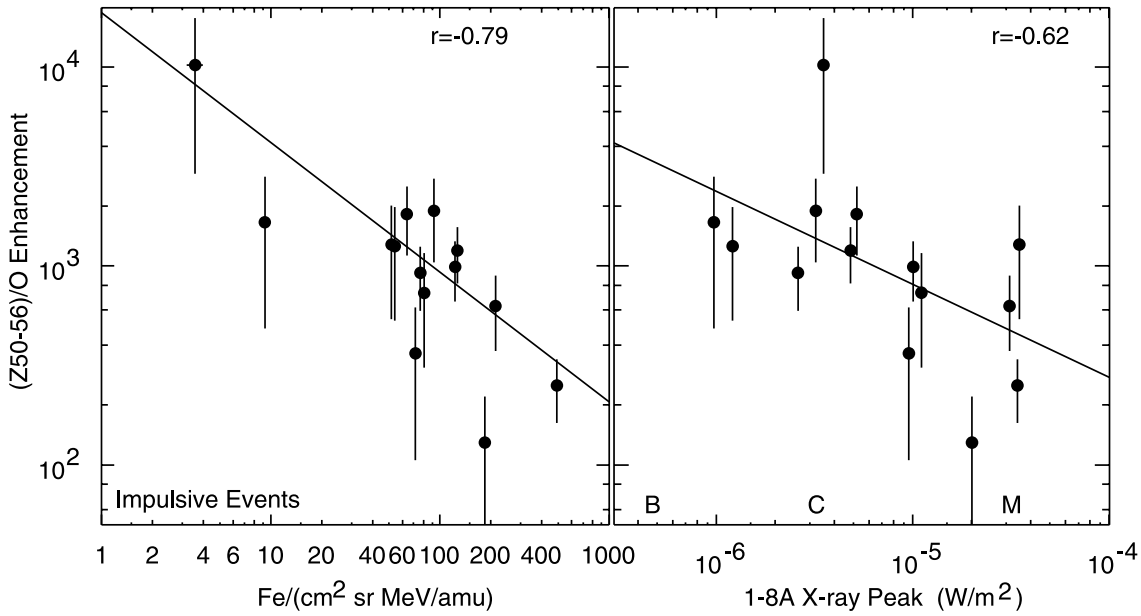

FIG. 8.—Enhancements in the $(50 \leq Z \leq 56)/\mathrm{O}$ abundances, plotted as a function of the 2.4–3.2 MeV amu^{-1} fluence of Fe (*left*) and the *GOES* soft X-ray peak flux (*right*) for the large impulsive events in which the abundances are well determined. Least-squares fit lines and correlation coefficients are shown.

at three different solar longitudes, show enhancements in $(34 \leq Z \leq 40)/\mathrm{O}$ that are only modestly larger than those in Fe/O and have a similar time dependence. Despite the high intensities of lighter ions in the large events in Figure 9, which exceed those of impulsive events by orders of magnitude (compare Fig. 2), ions with $Z \geq 50$ are sufficiently rare that we cannot follow their time dependence. Data leading to similar conclusions have been shown in other gradual events (Reames 2000; Reames et al. 2001).

In Figure 10 we show the time-integrated heavy-element enhancements as a function of the enhancement of Fe/O for the sample of 48 large gradual SEP events defined above. Here the average enhancement factors are quite modest, in contrast to those for impulsive events shown in Figure 3. The $(34 \leq Z \leq 40)/\mathrm{O}$ enhancements shown in Figure 10 are correlated with those of Fe/O with a correlation coefficient $r = 0.86$, and the least-squares fit line passes close to the unenhanced coronal abundances for both species. Strong correlation of element abundances in gradual SEP events is common (e.g., Reames 1995a, 1999). The heavier elements in Figure 10 are sufficiently rare, despite the high fluence of Fe ions, that correlations cannot be established. Upper limits on the enhancements of $Z \geq 34$ ions are suppressed in Figure 10 but are listed in Table 2; these limits confine the enhancements to very modest values. Analysis of the time evolution of the large gradual events suggests that some of the $Z \geq 50$ ions arrive late in the events, after the time of shock passage when they might come from small impulsive SEP events that are otherwise obscured by high intensities of elements with $Z \leq 26$ (an example occurs during the event of 2001 November 23 shown in Fig. 9).

5. DISCUSSION

The overall pattern of the intensities of Fe, O, and other species in the region of ~1–10 MeV amu^{-1} supports the earlier findings (Reames 1988) of a bimodal distribution reflecting both impulsive and gradual SEP events. The two classes of events are clearly present, although they are not fully resolved by Fe/O alone. These event classes, originally distinguished by the timescale of the associated soft X-ray events, have come to differentiate the effects of the physical mechanism of resonant stochastic acceleration in flares from those of shock acceleration at CME-driven shock waves (Reames 1999, 2002).

Variations of abundances with energy may cause patterns that are obvious in our energy region to become obscured in other regions. Differences in the spectral indexes of different species that we see will cause abundance variations to be greatly magnified at higher energies. When we attempt to replot Figure 1 using O and Fe intensities near 10 MeV amu^{-1}, we find that the distinction between impulsive and gradual events becomes blurred and loses its bimodal character. Therefore, *abundances measured above 10 MeV amu^{-1} may be completely useless in distinguishing impulsive and gradual SEP events*.

There are certainly mechanisms that could blur the resolution of impulsive and gradual events at other energies. Below 1 MeV amu^{-1}, abundances may be strongly affected by differing transport (e.g., Ng et al. 2003) and magnetic connections (Mazur et al. 2000) during the long transit times of many hours or days from the source to the observer. Above 10 MeV amu^{-1}, energy-dependent differences in the trapping and acceleration of ions in the source region must become important. Perhaps these same mechanisms cause the abundances to vary with energy, as we observe. However, poor discrimination of impulsive and gradual events at other energies does not negate the bimodal abundance pattern that we have seen for three solar cycles in the region of a few MeV amu^{-1}.

When we examine the heavy-element events listed by Mason et al. (2004), we find that many of the events have low values of $^3\mathrm{He}/^4\mathrm{He}$ (<0.01) and Fe/O (<0.5). We believe these are likely to be gradual events, although criteria may differ in the 0.1–1.0 MeV amu^{-1} region. If we focus on the nine events listed with positive measurements of $(m > 100)/\mathrm{Fe}$ (and enhancement factors of 600–5000), all have $\mathrm{Fe/O} > 1$ (1.49–4.55) and are surely impulsive events. Of these, five are also

TABLE 2

LARGE GRADUAL SEP EVENTS

Event	SEP Onset Time	Fe Fluence[a] (cm^{-2} sr^{-1} MeV^{-1} amu)	Fe/O Enhancement[b]	$(34 \leq Z \leq 40)$/O Enhancement[c]	$(50 \leq Z \leq 56)$/O Enhancement[d]	$(76 \leq Z \leq 82)$/O Enhancement[e]
1.....	1997 Nov 6 1400	2530 ± 14	3.15 ± 0.02	7.7 ± 1.3	8.2 ± 3.7	<4.7
2.....	1998 Apr 20 1200	6200 ± 19	2.14 ± 0.01	2.59 ± 0.25	0.36 ± 0.26	<0.52
3.....	1998 Aug 24 2300	574 ± 7	0.393 ± 0.004	0.275 ± 0.19	<1.1	<3.0
4.....	1998 Sep 23 1200	22.7 ± 1.1	0.461 ± 0.022	4.6 ± 4.6	<36	<10
5.....	1998 Sep 30 1400	3110 ± 21	1.63 ± 0.01	2.66 ± 0.58	1.9 ± 1.4	<2.8
6.....	1998 Nov 5 2200	116 ± 4	0.504 ± 0.017	<2.5	19 ± 19	54 ± 54
7.....	1998 Nov 14 0700	1030 ± 9	3.7 ± 0.03	7.1 ± 1.8	10.2 ± 5.9	9.7 ± 9.7
8.....	1999 Apr 24 1500	68.1 ± 2.7	0.673 ± 0.024	11.4 ± 11.4	<87	<250
9.....	1999 May 3 1200	41.5 ± 1.9	0.155 ± 0.007	<1.6	<12	<36
10.....	1999 Jun 4 0900	651 ± 7	0.8 ± 0.009	1.39 ± 0.70	<2.7	<7.6
11.....	2000 Apr 4 1700	353 ± 6	0.476 ± 0.007	<0.46	3.5 ± 3.5	<10.
12.....	2000 Jun 6 1900	113 ± 4	0.147 ± 0.005	<0.75	<5.8	<17
13.....	2000 Jul 14 1100	20500 ± 47	3.51 ± 0.01	22.7 ± 1.9	4.8 ± 2.4	<3.4
14.....	2000 Sep 12 1300	663 ± 9	0.241 ± 0.003	0.18 ± 0.18	<1.4	<4.0
15.....	2000 Nov 8 2300	40100 ± 109	3.22 ± 0.01	15.5 ± 1.8	3.0 ± 2.1	4.3 ± 4.3
16.....	2000 Nov 24 0600	1120 ± 10	1.06 ± 0.009	1.7 ± 0.7	<1.9	<5.4
17.....	2001 Jan 28 1800	182 ± 4	1.83 ± 0.04	3.0 ± 3.0	<23	<65
18.....	2001 Mar 25 1200	24.3 ± 1.2	0.402 ± 0.021	4.8 ± 4.8	<37	<105
19.....	2001 Mar 29 1200	433 ± 6	3.36 ± 0.04	3.7 ± 2.1	<9.5	<27
20.....	2001 Apr 3 0000	4820 ± 24	2.35 ± 0.01	4.2 ± 0.7	2.5 ± 1.5	<2.4
21.....	2001 Apr 10 1000	1410 ± 13	0.887 ± 0.008	0.49 ± 0.34	<1.9	<5.3
22.....	2001 Apr 15 1400	2630 ± 17	2.56 ± 0.017	1.97 ± 0.74	4.3 ± 3.1	<6.2
23.....	2001 Apr 18 0400	583 ± 7	1.57 ± 0.016	0.9 ± 0.6	<3.5	<10
24.....	2001 May 7 1300	178 ± 3	1.4 ± 0.02	<1.4	<11	<31
25.....	2001 Aug 9 1900	99.4 ± 2.9	0.335 ± 0.010	<1.2	<9.2	<26
26.....	2001 Aug 16 0100	257 ± 4	1.34 ± 0.017	0.93 ± 0.66	<3.6	<10
27.....	2001 Sep 24 1100	6010 ± 31	0.958 ± 0.0046	1.39 ± 0.27	0.39 ± 0.39	<1.1
28.....	2001 Oct 1 1300	1340 ± 11	0.535 ± 0.0039	0.58 ± 0.21	0.56 ± 0.55	<1.6
29.....	2001 Nov 4 1400	5840 ± 26	2.52 ± 0.011	4.01 ± 0.64	3.2 ± 1.6	<2.3
30.....	2001 Nov 17 0800	31.8 ± 1.6	0.167 ± 0.010	<2.4	<18	<53
31.....	2001 Nov 22 1800	12600 ± 42	1.09 ± 0.004	1.78 ± 0.23	<0.23	<0.66
32.....	2001 Dec 26 0600	2060 ± 15	1.51 ± 0.01	2.24 ± 0.65	<1.4	<4.1
33.....	2001 Dec 30 1900	1090 ± 9	0.649 ± 0.005	0.725 ± 0.32	<1.1	3.2 ± 3.2
34.....	2002 Jan 10 1600	71.6 ± 2.5	0.111 ± 0.004	<0.64	<4.9	<14
35.....	2002 Mar 16 0200	299 ± 5	0.369 ± 0.007	<0.69	<5.3	<15
36.....	2002 Mar 18 0600	296 ± 6	0.717 ± 0.016	<1.34	<10	<29
37.....	2002 Mar 22 1400	19.5 ± 1.3	0.0387 ± 0.0036	<1.75	<13	<38
38.....	2002 Apr 17 0700	116 ± 3	0.511 ± 0.015	<1.66	<13	<37
39.....	2002 Apr 21 0200	9330 ± 30	1.3 ± 0.004	2.59 ± 0.27	0.43 ± 0.30	<0.61
40.....	2002 May 22 1200	314 ± 6	0.282 ± 0.005	1.41 ± 0.70	<2.7	<7.7
41.....	2002 Jul 16 0900	307 ± 6	0.5 ± 0.010	1.38 ± 0.98	15.9 ± 9.2	<15
42.....	2002 Jul 22 0000	331 ± 5	0.614 ± 0.008	0.36 ± 0.36	<2.8	<7.9
43.....	2002 Aug 14 0300	72.8 ± 2.3	0.467 ± 0.015	1.9 ± 1.9	<14	<41
44.....	2002 Aug 24 0600	1610 ± 12	1.16 ± 0.008	1.65 ± 0.55	<1.4	<4.0
45.....	2002 Sep 5 2300	67.2 ± 2.1	0.495 ± 0.015	<1.57	<12	<35
46.....	2002 Nov 9 1600	898 ± 7	0.936 ± 0.008	0.93 ± 0.46	1.8 ± 1.8	<5.1
47.....	2003 May 28 0500	971 ± 9	1.38 ± 0.014	0.98 ± 0.70	<3.8	<11
48.....	2003 Jun 18 0700	92.9 ± 2.5	0.21 ± 0.006	<0.67	<5.1	<15

[a] At 2.4–3.2 MeV amu^{-1}.
[b] At 3.3–10 MeV amu^{-1}, relative to coronal (Fe/O = 0.134).
[c] At 3.3–10 MeV amu^{-1}, relative to coronal $[(34 \leq Z \leq 40)/O = 2.22 \times 10^{-5}]$.
[d] At 3.3–10 MeV amu^{-1}, relative to coronal $[(50 \leq Z \leq 56)/O = 2.90 \times 10^{-6}]$.
[e] At 3.3–10 MeV amu^{-1}, relative to coronal $[(76 \leq Z \leq 82)/O = 1.01 \times 10^{-6}]$.

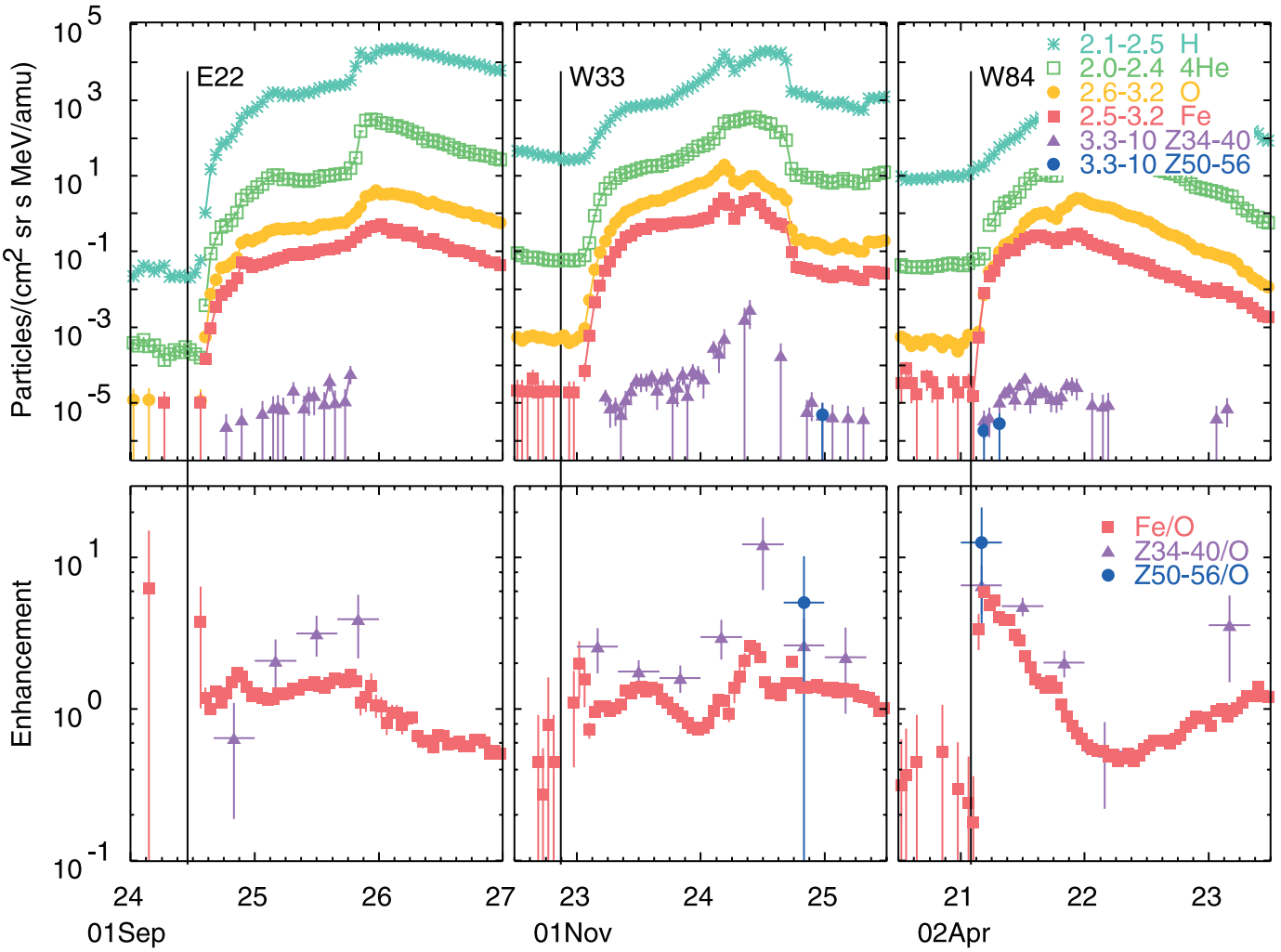

FIG. 9.—*Top panels*: Intensities of three large gradual events as a function of time. *Bottom panels*: Enhancements in the abundance ratios Fe/O, $(34 \leq Z \leq 40)$/O, and $(50 \leq Z \leq 56)$/O relative to coronal abundance ratios vs. time.

found on our list of 39 large impulsive events described above; the remaining four events show little or no increase in Fe above 2 MeV amu^{-1}, suggesting that these events have sufficiently steep spectra that they are too small to be seen at high energies. The Mason et al. (2004) list contains events with intensities of Fe > 0.1 ions cm^{-2} sr^{-1} s^{-1} MeV^{-1} amu above 100 keV amu^{-1}, while our final list contains events with intensities of Fe $> 10^{-4}$ ions cm^{-2} sr^{-1} s^{-1} MeV^{-1} amu above 2 MeV amu^{-1}. Small events with differential energy spectra steeper than $\sim E^{-4}$ could be seen by Mason et al. (2004) but not by us. The four events on the Mason et al. (2004) list that are too steep to be seen by LEMT include the three highest values of $(m > 100)$/Fe enhancement that they report, supporting our finding that the events with the steepest spectra have the greatest heavy-element enhancements. The five events that we have in common have Fe spectral indexes between -1.8 and -3.4.

The Fe spectral indexes of our 39 large impulsive events range from -1.8 to -4.4, with a mean value of -3.1. There is a correlation ($r = 0.81$) between the $(50 \leq Z \leq 56)$/O enhancement and the Fe spectral index, so that events with steeper Fe spectra have greater $(50 \leq Z \leq 56)$/O enhancements. Over the observed spectral range, enhancements vary from $\sim 10^2$ to $\sim 10^4$, and a similar range of enhancements is seen for $(76 \leq Z \leq 82)$/O. *Differences in spectra are an essential factor in the enhancement of heavy elements.* Furthermore, small events, as measured by the Fe fluence, have greater enhancements. The Fe spectral index is only weakly correlated ($r = 0.46$) with the Fe fluence for the 39 events.

Fe fluence is one measure of impulsive event size, and soft X-ray flux is another; both suggest that small events with less energy input have the greatest heavy-element enhancements. A similar result was found for enhancements in ^{3}He/^{4}He (Reames et al. 1988).

Qualitatively, the heavy-element and spectral behavior can be understood based on the model of cascading waves (e.g., Miller 1998), in which waves generated at long wavelengths (low wavenumber k), by magnetic reconnection in a flare, cascade toward higher k, passing through resonance with ions of increasing gyrofrequency or Q/A as they go. When the energy in waves is low, most of it can be absorbed by the ions at highest Z (lowest Q/A), causing greater enhancements but steeper spectra because of the limited available energy, especially at lower Z. In larger flares more energy is available to produce harder spectra, and wave absorption by the limited numbers of heavy ions is inadequate to stem the flood of cascading waves. Unfortunately, however, we do not yet have a quantitative model that explains the full range of observations.

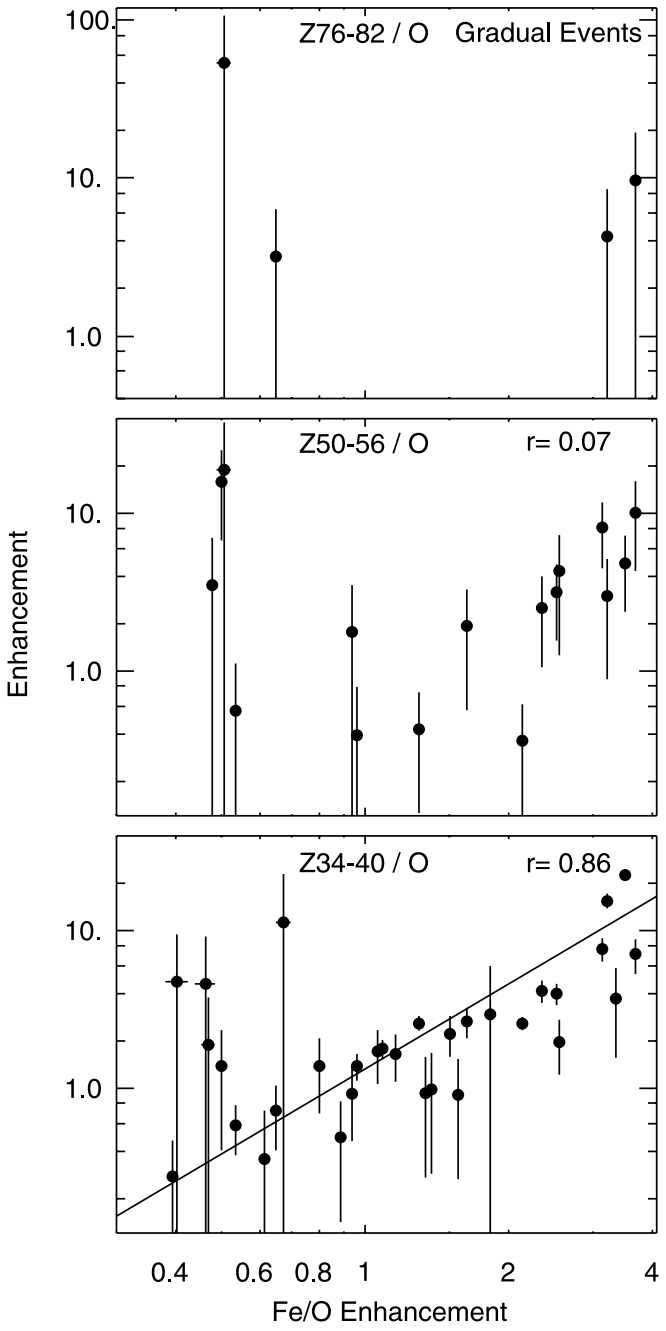

FIG. 10.—Enhancements in the heavy-element abundance ratios ($34 \leq Z \leq 40$)/O, ($50 \leq Z \leq 56$)/O, and ($76 \leq Z \leq 82$)/O relative to coronal abundance ratios, shown vs. the corresponding enhancement in Fe/O for a sample of 48 large gradual events. The correlation coefficients (r) and least-squares fit lines are shown in the bottom panel. Average enhancements are *substantially* smaller in these gradual events than in the impulsive events shown in Fig. 3.

The above arguments suggest that saturation in the magnitude of heavy-element enhancements becomes important as the flare energy increases. In the flare plasma, there are only approximately two ions with $50 \leq Z \leq 56$ for every 10^{10} H ions (Grevesse & Sauval 1998). Ultimately, once all the $Z \geq 50$ ions in the flare volume have been accelerated, additional energy can only go into lighter ions, so the enhancements begin to decrease. This kind of saturation of heavy-element enhancements may explain why enhancements in ($76 \leq Z \leq 82$)/O do not exceed those in ($50 \leq Z \leq 56$)/O. Depletion of ^{3}He in the flare volume has been invoked to explain the systematic decrease in ^{3}He/^{4}He in impulsive SEP events with increasing particle fluences (Reames 1999). With reasonable approximations, the number of energetic ^{3}He ions in space was found to be a significant fraction of the number available in a flare volume. Although the abundance of ^{3}He exceeds that of $Z \geq 50$ ions in the flare plasma, ^{3}He is presumably accelerated preferentially because it resonates with electromagnetic ion cyclotron waves that peak near the ^{3}He gyrofrequency (Temerin & Roth 1992; Roth & Temerin 1997), while the acceleration of $Z \geq 50$ ions involves cascading Alfvén turbulence.

The strong coupling between spectra and abundances in impulsive SEP events, seen for both ^{3}He (Mason et al. 2002) and $Z \geq 50$, seems to argue against a two-phase process (e.g., Fisk 1978) in which a selective heating mechanism determines the enhancements while a separate acceleration mechanism determines the spectra. The observations seem to favor acceleration and enhancement of all ions by a single resonant process, although different wave modes may resonate preferentially with different ions.

6. CONCLUSIONS

Element abundances of 2–10 MeV amu^{-1} ions from SEP events show a bimodal pattern reflecting the underlying contributions of impulsive and gradual SEP events that result from two different acceleration mechanisms. Flare-associated impulsive events have enhancements in ions with $Z \geq 50$ by factors of 100–10,000 relative to coronal abundances, while the corresponding enhancements in the shock-accelerated particles from gradual events are only 0.2–20.

The enhancements in $Z \geq 50$ ions in impulsive events are uncorrelated with Fe/O but are strongly correlated with the energy spectral index of Fe, with the Fe fluence, and with the soft X-ray flux from the flare. Smaller events and those with steeper energy spectra have greater heavy-element enhancements. This suggests that when the flare energy available for acceleration is small, much of it is absorbed first by rare heavy elements (and ^{3}He), leaving only enough to produce steep energy spectra for the more abundant ions. As the energy input increases, the supply of heavy elements is depleted, and more energy flows into the abundant element species at higher Q/A, accelerating them in greater numbers with increasingly hard spectra.

We thank G. M. Mason for helpful discussions of the Mason et al. (2004) results.

REFERENCES

Arnaud, M., & Raymond, J. 1992, ApJ, 398, 394
Arnaud, M., & Rothenflug, R. 1985, A&AS, 60, 425
Desai, M. I., Mason, G. M., Mazur, J. E., Dwyer, J. R., Gold, R. E., Krimigis, S. M., Smith, C. W., & Skoug, R. M. 2003, ApJ, 588, 1149
Fisk, L. A. 1978, ApJ, 224, 1048
Gosling, J. T. 1993, J. Geophys. Res., 98, 18937
Grevesse, N., & Sauval, A. J. 1998, Space Sci. Rev., 85, 161
Kahler, S. W. 1992, ARA&A, 30, 113
———. 1994, ApJ, 428, 837
———. 1997, in Coronal Mass Ejections, ed. N. Crooker, J. A. Jocelyn, & J. Feynman (Geophys. Monogr. 99; Washington, DC: AGU), 227
———. 2001, J. Geophys. Res., 106, 20947

Mason, G. M., Mazur, J. E., & Dwyer, J. R. 1999, ApJ, 525, L133
Mason, G. M., Mazur, J. E., Dwyer, J. R., Jokipii, J. R., Gold, R. E., & Krimigis, S. M. 2004, ApJ, 606, 555
Mason, G. M., et al. 2002, ApJ, 574, 1039
Mazur, J. E., Mason, G. M., Dwyer, J. R., Giacalone, J., Jokipii, J. R., & Stone, E. C. 2000, ApJ, 532, L79
Meyer, J. P. 1985, ApJS, 57, 151
Miller, J. A. 1998, Space Sci. Rev., 86, 79
Miller, J. A., & Viñas, A. F. 1993, ApJ, 412, 386
Ng, C. K., Reames, D. V., & Tylka, A. J. 1999, Geophys. Res. Lett., 26, 2145
———. 2003, ApJ, 591, 461
Post, D. E., Jensen, R. V., Tarter, C. B., Grasberger, W. H., & Lokke, W. A. 1977, At. Data Nucl. Data Tables, 20, 397
Reames, D. V. 1988, ApJ, 330, L71
———. 1990, ApJS, 73, 235
———. 1995a, Adv. Space Res., 15, 41
———. 1995b, Rev. Geophys. Suppl., 33, 585
———. 1999, Space Sci. Rev., 90, 413
———. 2000, ApJ, 540, L111
Reames, D. V. 2002, ApJ, 571, L63
Reames, D. V., Barbier, L. M., von Rosenvinge, T. T., Mason, G. M., Mazur, J. E., & Dwyer, J. R. 1997, ApJ, 483, 515
Reames, D. V., Dennis, B. R., Stone, R. G., & Lin, R. P. 1988, ApJ, 327, 998
Reames, D. V., & McDonald, F. B. 2003, ApJ, 586, L99
Reames, D. V., Meyer, J. P., & von Rosenvinge, T. T. 1994, ApJS, 90, 649
Reames, D. V., Ng, C. K., & Tylka, A. J. 2000, ApJ, 531, L83
———. 2001, ApJ, 548, L233
Roth, I., & Temerin, M. 1997, ApJ, 477, 940
Shirk, E. K., & Price, B. P. 1973, Proc. 13th Int. Cosmic Ray Conf. (Denver), 2, 1474
Temerin, M., & Roth, I. 1992, ApJ, 391, L105
Tylka, A. J. 2001, J. Geophys. Res., 106, 25333
Tylka, A. J., Boberg, P. R., Cohen, C. M. S., Dietrich, W. F., Maclennan, C. G., Mason, G. M., Ng, C. K., & Reames, D. V. 2002, ApJ, 581, L119
Tylka, A. J., Cohen, C. M. S., Dietrich, W. F., Maclennan, C. G., McGuire, R. E., Ng, C. K., & Reames, D. V. 2001, ApJ, 558, L59
Tylka, A. J., Reames, D. V., & Ng, C. K. 1999, Geophys. Res. Lett., 26, 2141
von Rosenvinge, T. T., et al. 1995, Space Sci. Rev., 71, 155